4、Generic Adaptive Sliding Mode Control for a Quadrotor UAV System Subject to Severe Parametric Uncertainties and Fully Unknown External Disturbance

单位/学校	西南交通大学
院系、专业及研究方向	电气工程学院、无人机控制与路径规划
论文发表在何期刊	Complexity
期刊索引情况	SCI
影响因子	2.462
论文内容简介	针对四旋翼无人机受到的参数不确定性和外部扰动的问题，本文提出一种鲁棒自适应滑模控制技术。首先，基于牛顿-欧拉方程建立四旋翼无人机的欠驱动动力学模型。然后，使用滑模方法设计四旋翼无人机的高度和姿态的控制律。同时，提出一种群参数自适应律估计四旋翼无人机动力学模型的所有物理参数。利用 Lyapunov 定理证明了所提控制器能够渐进删除跟踪误差。最后，通过与自抗扰控制器、线性二次调节器的仿真与实验对比，说明了所提控制器的有效性和鲁棒性。
论文创新内容与工程应用价值	本文的创新在于提出一种群参数自适应律估计四旋翼无人机的所有物理参数。所设计的控制器能够应用于任何种类的四旋翼无人机。此外，借助灵思创奇公司提供的实验台架，我们通过对比实验验证了所设计的控制器在追踪性能上优于自抗扰控制器和线性二次调节器。因此，我们的研究具有重要的工程价值
灵思创奇设备价值	本文的实验验证基于灵思创奇公司提供的四旋翼无人机实验台架。首先，在 MATLAB/Simulink 中完成控制器的搭建与仿真验证。然后，借助灵思创奇公司提供的上位机软件，利用 MATLAB 中的代码生成技术将 Simulink 中的控制器模块转化为 C 语言，并利用 WIFI 将其下载到无人机的控制芯片中。最后，调试控制参数完成实验验证。 这套设备的价值在于它帮助研究人员避免了 C 语言的编写，把更多的时间投入到高效、可靠的控制器设计中。因此，它极大地缩短了研究人员在无人机上验证所设计的控制器的时间。

International Journal of Control, Automation and Systems 19(2) (2021) 698-711
http://dx.doi.org/10.1007/s12555-019-0853-3 ISSN:1598-6446 eISSN:2005-4092
http://www.springer.com/12555

Generic Adaptive Sliding Mode Control for a Quadrotor UAV System Subject to Severe Parametric Uncertainties and Fully Unknown External Disturbance

Tianpeng Huang, Deqing Huang*, Zhikai Wang, Xi Dai, and Awais Shah

Abstract: This paper aims to provide a generic robust controller that is able to manipulate all kinds of quadrotor unmanned aerial vehicle (UAV) systems automatically or adaptively in the presence of severe parametric uncertainties and fully unknown external disturbance. The dynamic model of the quadrotor is first obtained using Newton-Euler equations. Then, considering the underactuated and the strongly coupled characteristics of the quadrotor system, a nonlinear adaptive sliding mode control (ASMC) scheme is proposed. Meanwhile, additional adaptive laws are designed to estimate all the parameters of the quadrotor system, which in principle are difficult to be measured directly and accurately. Furthermore, to guarantee the asymptotic stability of the closed-loop system, the upper bound of the fully unknown external disturbance is estimated and adopted as the switching gain of the ASMC. Finally, simulations and experiments are carried out to illustrate the effectiveness and robustness of the proposed control scheme, where the superiority to linear quadratic control (LQR) and active disturbance rejection control (ADRC) has been demonstrated clearly.

Keywords: Adaptive sliding mode controller, external disturbance, parametric uncertainty, quadrotor unmanned aerial vehicle.

1. INTRODUCTION

The attention of quadrotor UAVs has gradually increased in civilian and commercial applications recently as they have several advantages over the fixed-wing aircrafts and the traditional-rotor helicopters including the ability to hover, quite simplified mechanical design, maneuverability and vertical takeoff and landing [1–3].

To meet the requirement of flight mission with high reliability, the design of specialized controller for a quadrotor UAV in both indoor and outdoor environments is indispensable. However, the control of quadrotor is still a challenging work due to underactuated characteristics, modeling nonlinearity with strongly coupled dynamics as well as the effect of large payload variation, gyroscopic moments. In addition, external disturbances and uncertainty of parameters are ubiquitous phenomena in the design of quadrotor controller, which have been highlighted in the literatures over the years.

First, for the quadrotor system subject to parametric uncertainties, [4] presents a closed-form nonlinear control strategy for achieving tracking of desired output of translational movement in a quadrotor aerial vehicle model with uncertain physical parameters, including mass and inertia moment. In [5], to solve the problem of safe and fast delivery of packages by a quadrotor, a control technique based on the interconnection and damping assignment is proposed despite the uncertainties of moments of inertia and mass of the quadrotor. Meanwhile, adaptive control scheme has been widely used in four-rotor UAV system with parametric uncertainties [6–9]. More specifically, a robust adaptive attitude dynamics controller is developed in [6] to asymptotically follow a given attitude command and an adaptive law is designed simultaneously for estimating the inertia matrix for the quadrotor dynamics. In [7], the backstepping control is employed to settle the under-actuation issue of the four-rotor aircraft, while adaptive learning algorithm is applied to real-time estimation of mass parameter of the quadrotor. In [8], an immersion and invariance adaptation scheme is designed to allow the estimated mass of the four-rotor system to converge to its real value asymptotically. To ensure finite-time

Manuscript received October 8, 2019; revised January 3, 2020 and March 22, 2020; accepted May 4, 2020. Recommended by Associate Editor Choon Ki Ahn under the direction of Editor Chan Gook Park. The work was supported by the Sichuan Science and Technology Program under Grant 2019YFG0345, Grant 2019YJ0210, the National Natural Science Foundation of China under Grant 61773323, Grant U1934221, Grant 61733015.

Tianpeng Huang, Deqing Huang, Zhikai Wang, Xi Dai, and Awais Shah are with the School of Electrical Engineering, Southwest Jiaotong University, Chengdu, China (e-mails: tphuang@my.swjtu.edu.cn, elehd@home.swjtu.edu.cn, {zhikaiwang, dayhee, Awaisshah}@my.swjtu.edu.cn).
* Corresponding author.

stabilization of quadrotor, [9] provides a construction approach of ASMC, where the proper adaptive algorithms are adopted to estimate the uncertain physical factors of the quadrotor. However, the ability to reject external disturbances is not considered in the ASMC when system stability is analyzed.

Then, for the quadrotor UAV system with external disturbances, backstepping control has been extensively studied to address the problem of trajectory tracking [10, 11]. In particular, in [12], to robustly reject external constant and unknown stochastic disturbances, a nonlinear control law consisting of SMC and backstepping control method is introduced to track the reference signal of the translation subsystem and rotation subsystem of a quadrotor helicopter. In [13], a second-order SMC scheme is investigated and implemented on a four-rotor helicopter, which has demonstrated robustness to disturbances. In addition, [14] suggests a hybrid control algorithm that incorporates optimal LQR and robust SMC to achieve the velocity following of a small-scale unmanned aircraft system under the perturbation effects. A continuous SMC strategy with uniform exponential stability is proposed in [15, 16] to realize the trajectory tracking task of the translational and rotational motion of a four-rotor aircraft subject to the influence of some kind of disturbances. [17] presents a robust nonlinear control methodology, which is actually applied to a four-rotor unmanned system, for trajectory tracking and waypoint navigation in consideration of external wind gusts disturbance. In [18], external force and torque are taken as disturbances to the system and are estimated by the designed observers. Further, a nonlinear controller with the estimated values by the observers is developed to compensate the external disturbances and to achieve the stable control of the position loop and attitude loop of the four-rotor system. In [19], to design robust H_∞ controller to stabilize the nonlinear quadrotor system suffering various external disturbances, a systematic method based on linear matrix inequality is proposed. Meanwhile, [20] introduces a new nonlinear control law with exponential convergence for the trajectory tracking of translational and rotational movement of four-rotor systems that do not have any simplified information and assumption of model. In [21], a robust attitude stabilization algorithm based on switching model predictive is presented for a four-rotor unmanned system taking into account atmospheric disturbances. [22] develops an anti-Gaussian random disturbance control strategy to achieve the path following of a quadrotor system.

Furthermore, many studies have been done to achieve the robust control of four-rotor UAV under the coupling effect of external disturbances and parametric uncertainties. In [23], a model predictive controller is presented to complete the path following in the position subsystem, while a nonlinear H_∞ strategy is proposed to control the attitude subsystem for a four-rotor aircraft in the case of sustained external slight gust and the uncertainties of mass and inertia matrix. To realize that a four-rotor aircraft can follow the preset location point and pose point under the consideration of drag coefficients uncertainty and external disturbances, a robust guaranteed cost control scheme is introduced in [24]. [25] proposes a nonlinear control approach to overcome the total uncertainty, which incorporates external disturbances, parameters and unmodeled uncertainty for robustly stabilizing the three attitude angles of a quad-rotor UAV system. In [26], a control strategy combining adaptive control and saturation control is investigated to achieve path tracking of a four-rotor aircraft in translational and rotational motion, which has considered additional external disturbances, uncertainty of drag coefficient and moment of inertia parameters. Besides, [27] proposes a dynamic surface based robust control technique for a four-rotor aircraft under the influence of uncertainty of parameters including damping matrices, arm length, force-to-moment factor and unknown external lumped disturbances online estimated by extended state observer. Meanwhile, a novel nonlinear internal model controller and a multivariable super-twisting-like algorithm are presented in [28] and [29] respectively to achieve the tracking control of attitude loop of a four-rotor aircraft in the face of wind gust and uncertainty of inertia matrix. Furthermore, to achieve control of position and attitude of quadrotor, an adaptive nonsingular fast terminal SMC and an adaptive backstepping fast terminal SMC are designed in [30] and [31], respectively. The robustness of the ASMC schemes developed in [30, 31] to external disturbance and uncertainty of physical parameters has been verified by simulation experiments. In [32], a robust ASMC approach is developed for attitude and altitude tracking of a four-rotor system under the simultaneous effect of parametric uncertainties and consistent external disturbance. This ASMC can only deal with external disturbance with known upper bound. In [33], a saturated ASMC is suggested to address autonomous vessel landing problem for a quadrotor considering parameter uncertainty and external disturbances. [34] presents a neural network-based ASMC design for control of a quadrotor, which provides disturbance rejection capability and is insensitive to parameters. However, the ASMC methods employed in [33, 34] only consider uncertainties of partial parameters of quadrotor UAV system.

It is worth highlighting that, although numerous works have been reported for controller design of quadrotor system when parametric uncertainties and/or external disturbance are involved, there are no generic robust controllers that are able to manipulate all kinds of quadrotors automatically or adaptively under the impact of severe parametric uncertainties and fully unknown external disturbance. Motivated by this and inspired by [9, 33, 34], a robust ASMC law is developed in this paper, which stabilizes the altitude and attitude tracking errors asymptotically. The main contributions of the paper are summarized as follows: 1) Unlike the existing results such as [6–8,27,33,34] that estimate partial parameters of quadrotor, in this paper, to deal with the severe parametric uncertainties in a generic way, all the parameters of the system are estimated efficiently via the designed adaptive laws, which allow the proposed controller to be applied to any type of quadrotor system. 2) The asymptotical stability of the control laws is proven rigorously, when the fully unknown external disturbance is involved. 3) The robustness and effectiveness of the proposed controller have been verified via simulations, real experiments and comparison with LQR [35] and ADRC [36].

The remainder of this paper is organized as follows: The description of mathematical model of the quadrotor and problem statement are given in Section 2. Section 3 introduces the proposed controller and its stability analysis. In Section 4, the simulation results and actual experiment results are presented, respectively. Finally, the main conclusions of the paper and direction of future work are presented in Section 5.

2. DYNAMICS DESCRIPTION AND PROBLEM STATEMENT

2.1. Dynamic model of the quadrotor

We consider the dynamic model of the quadrotor system and its detailed derivation process. The actual quadrotor is shown in Fig. 1, where E and B represent the earth and body frames, respectively.

As usual, the following assumptions are given to make the consequent controller design and analysis rigorous [9, 10, 37].

- The earth frame is the inertial frame.
- The structure of the quadrotor UAV is symmetrical.

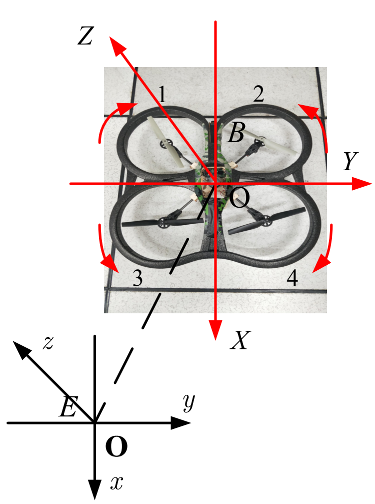

Fig. 1. Quadrotor UAV.

- The structure of the quadrotor UAV is rigid, and there are no internal forces or deformations.

Let $[x, y, z]$ denotes the three-degree-of-freedom position state of output of the quadrotor and $[\phi, \theta, \varphi]$ represents the three-degree-of-freedom attitude state of output of the quadrotor, where ϕ is the roll angle around the x-axis, θ the pitch angle around the y-axis as well as φ the yaw angle around the z-axis in the coordinate system E.

The rotation matrices around each of the three axes from earth frame to body frame are given as:

$$R_\phi = \begin{bmatrix} 1 & 0 & 0 \\ 0 & \cos\phi & \sin\phi \\ 0 & -\sin\phi & \cos\phi \end{bmatrix}, \tag{1}$$

$$R_\theta = \begin{bmatrix} \cos\theta & 0 & -\sin\theta \\ 0 & 1 & 0 \\ \sin\theta & 0 & \cos\theta \end{bmatrix}, \tag{2}$$

$$R_\varphi = \begin{bmatrix} \cos\varphi & \sin\varphi & 0 \\ -\sin\varphi & \cos\varphi & 0 \\ 0 & 0 & 1 \end{bmatrix}. \tag{3}$$

Then, the transition matrix from system B to system E is obtained by

$$R_{BE} = (R_\phi R_\theta R_\varphi)^T, \tag{4}$$

where $(\cdot)^T$ is transpose of matrix $(\cdot)$.

In the following, the translational and rotational dynamics of the four-rotor system will be exploited consequently. First address the translational dynamics. Notice that the total lift force generated by the rotors can be given in the body frame as

$$F_T^b = [0, 0, U_1]^T, \tag{5}$$

with $U_1 \triangleq (F_1 + F_2 + F_3 + F_4)$ being the actual altitude control input, where F_i is the lift force generated by the ith rotor, $i = 1, \cdots, 4$. According to (4) and (5), the total lift force in the earth frame is then

$$F_l^e = R_{BE} F_T^b. \tag{6}$$

Meanwhile, the air resistance is proportional to the flight speed of quadrotor and can be expressed as

$$F_r^e = [k_x \dot{x}, k_y \dot{y}, k_z \dot{z}]^T, \tag{7}$$

where k_x, k_y and k_z are the air resistance coefficients in the three directions. Moreover, the effect of gravity of the quadrotor can be described in the coordinate system E as

$$F_g^e = [0, 0, mg]^T, \tag{8}$$

where m is the mass of quadrotor. In summary, applying Newton's second law, the translational dynamics of the quadrotor UAV subjected to external disturbance can be obtained by (1)-(8) [15,21].

$$\ddot{x} = \frac{U_1(\sin\theta\cos\phi\cos\varphi + \sin\phi\sin\varphi) - k_x\dot{x}}{m} + d_x,$$
$$\ddot{y} = \frac{U_1(\sin\theta\cos\phi\sin\varphi - \sin\phi\cos\varphi) - k_y\dot{y}}{m} + d_y,$$
$$\ddot{z} = \frac{U_1(\cos\phi\cos\theta) - k_z\dot{z} - mg}{m} + d_z, \tag{9}$$

where the d_x, d_y and d_z denote the effect of external wind disturbance on the translational motion of the quadrotor.

Then, the rotational dynamics of four-rotor system is addressed. Let $[p,q,r]$ represent the quadrotor's angular velocity in the coordinate system B. The differential equations of the angular motion of the quadrotor are given by [28,38]

$$M_x = J_x\dot{p} + (J_z - J_y)qr,$$
$$M_y = J_y\dot{q} + (J_x - J_z)pr,$$
$$M_z = J_z\dot{r} + (J_y - J_x)pq, \tag{10}$$

where M_x, M_y, M_z are the components of the resultant torque acting on the quadrotor in the three directions of x, y, z, respectively and J_x, J_y, J_z are the inertias of the quadrotor around x, y, z, respectively.

Meanwhile, let M_{lx}, M_{ly}, M_{lz} denote the components of the lifting torque of the quadrotor in the three directions of x, y, z, respectively. They can be expressed as [39]

$$M_{lx} = LU_2,$$
$$M_{ly} = LU_3,$$
$$M_{lz} = fU_4, \tag{11}$$

where L is the arm length of quadrotor and f is the scaling factor from force to moment. In addition, U_2, U_3, and U_4 are attitude control inputs and defined as $U_2 \triangleq (F_1 + F_3 - F_2 - F_4)$, $U_3 \triangleq (F_3 + F_4 - F_1 - F_2)$ and $U_4 \triangleq (F_1 + F_4 - F_2 - F_3)$, respectively.

Besides, the quadrotor is subject to gyroscopic torque during flight, whose components M_{gx}, M_{gy}, M_{gz} around the x, y, and z axes, respectively, are given by [39]

$$M_{gx} = J_r q\Omega_{11},$$
$$M_{gy} = J_r p\Omega_{11},$$
$$M_{gz} = 0. \tag{12}$$

In (12), J_r is the inertia of each propeller and $\Omega_{11} \triangleq \Omega_2 + \Omega_3 - \Omega_1 - \Omega_4$, where $\Omega_i, i = 1, \cdots, 4$ represents the angular speed of the ith propeller.

Considering (10)-(12), the angular motion dynamics of the quadrotor can be rewritten in the following form.

$$J_x\dot{p} = (J_y - J_z)qr - J_r q\Omega_{11} + LU_2,$$
$$J_y\dot{q} = (J_z - J_x)pr + J_r p\Omega_{11} + LU_3,$$
$$J_z\dot{r} = (J_x - J_y)pq + fU_4. \tag{13}$$

Compared with the brushless motor, the propeller is light. Hence, it is reasonable to ignore the moment of inertia caused by the propellers here [40]. Notice that the angular velocity $[p,q,r]$ in the coordinate system B can be converted to the angular velocity $[\dot{\phi}, \dot{\theta}, \dot{\varphi}]$ in the coordinate system E by [28,29]

$$\begin{bmatrix} \dot{\phi} \\ \dot{\theta} \\ \dot{\varphi} \end{bmatrix} = \begin{bmatrix} 1 & \sin\phi\tan\theta & \cos\phi\tan\theta \\ 0 & \cos\phi & -\sin\phi \\ 0 & \dfrac{\sin\phi}{\cos\theta} & \dfrac{\cos\phi}{\cos\theta} \end{bmatrix} \begin{bmatrix} p \\ q \\ r \end{bmatrix}. \tag{14}$$

To ensure flight safety, the attitude angles of the quadrotor are always kept small purposely during the flight. Thus, it follows from (14) that $[\dot{\phi}, \dot{\theta}, \dot{\varphi}]^T \approx [p,q,r]^T$ [41]. In consequence, the rotational dynamics of the quadrotor subjected to external disturbance [15,21] can be derived from (13),

$$\ddot{\phi} = \frac{(J_y - J_z)\dot{\theta}\dot{\varphi} - J_r\dot{\theta}\Omega_{11} + LU_2}{J_x} + d_\phi,$$
$$\ddot{\theta} = \frac{(J_z - J_x)\dot{\phi}\dot{\varphi} + J_r\dot{\phi}\Omega_{11} + LU_3}{J_y} + d_\theta,$$
$$\ddot{\varphi} = \frac{(J_x - J_y)\dot{\phi}\dot{\theta} + fU_4}{J_z} + d_\varphi, \tag{15}$$

where the d_ϕ, d_θ and d_φ represent the influence of external wind disturbance on the rotation motion of the quadrotor.

2.2. Problem statement

In the control of the quadrotor, the changes of the states ϕ and θ will result in movement in the x and y directions, respectively. Therefore, instead of considering the full six degrees of freedom of UAV, it is sufficient to control the four degrees of freedom (ϕ, θ, φ and z) only. Eventually, the considered quadrotor UAV system has a fully-actuated dynamic model [9], where the four independent control variables are to be designed.

Denote by z_d and $[\phi_d, \theta_d, \varphi_d]$ the desired altitude and the three desired attitude angles respectively. The central task is to design a tracking control strategy including an altitude control algorithm and an attitude control algorithm to ensure that the desired altitude and attitude trajectories can be followed asymptotically despite the severe parametric uncertainties and fully unknown external disturbance. In other words, by virtue of the proposed control scheme, the altitude tracking error $e_z = z_d - z$ and the attitude tracking error $e_\phi = \phi_d - \phi$, $e_\theta = \theta_d - \theta$, $e_\varphi = \varphi_d - \varphi$ are supposed to be stabilized and guaranteed to converge to zero.

3. CONTROLLER DESIGN AND STABILITY ANALYSIS

To accomplish the control design of the four-rotor UAV with high precision and high reliability under the influence

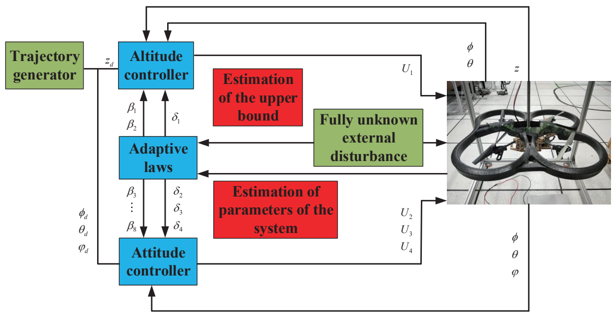

Fig. 2. Control scheme.

of parametric uncertainties and external disturbances, a robust ASMC is presented in this section, as shown in Fig. 2.

To make the subsequent analysis concise and readable, some of the involved disturbance components in (9) and (15) are rescaled as $\tilde{d}_z \triangleq md_z$, $\tilde{d}_\phi \triangleq (J_x/L)d_\phi$, $\tilde{d}_\theta \triangleq (J_y/L)d_\theta$, $\tilde{d}_\varphi \triangleq (J_z/f)d_\varphi$, and some of the parameters are redefined as $\beta_1 \triangleq m$, $\beta_2 \triangleq k_z$, $\beta_3 \triangleq J_x/L$, $\beta_4 \triangleq (J_y-J_z)/L$, $\beta_5 \triangleq J_y/L$, $\beta_6 \triangleq (J_z-J_x)/L$, $\beta_7 \triangleq J_z/f$, $\beta_8 \triangleq (J_x-J_y)/f$. Further, let $\hat{\beta}_i$ denote the estimation of β_i, $i=1,\cdots,8$. Then, $\tilde{\beta}_i \triangleq \beta_i - \hat{\beta}_i$ would be the estimation error.

Assumption 1: It is assumed that all the disturbances are uniformly bounded, i.e., $|d_x| \le \delta_x$, $|d_y| \le \delta_y$, $|\tilde{d}_z| \le \delta_1$, $|\tilde{d}_\phi| \le \delta_2$, $|\tilde{d}_\theta| \le \delta_3$, $|\tilde{d}_\varphi| \le \delta_4$ with unknown positive constant δ_x, δ_y, δ_1, δ_2, δ_3, δ_4.

Assumption 2: In the design of controller for the quadrotor, to avoid any singularity, we set [20]

$$-\frac{\pi}{2} < \phi < \frac{\pi}{2}, \tag{16a}$$
$$-\frac{\pi}{2} < \theta < \frac{\pi}{2}. \tag{16b}$$

3.1. Altitude controller design

The altitude controller is first designed. Set the sliding surface as

$$s_1 = c_1 e_z + \dot{e}_z, \tag{17}$$

with c_1 is a controller parameter to be designed and $c_1 > 0$.

The control input U_1 of altitude is designed as

$$\begin{aligned} U_1 =& \frac{1}{\cos\phi\cos\theta}(\hat{\beta}_1(c_1\dot{e}_z + \ddot{z}_d + g) + \hat{\beta}_2\dot{z} \\ &+ \hat{\delta}_1 sgn(s_1) + k_1 s_1), \end{aligned} \tag{18}$$

where $sgn(\cdot)$ denotes the signum function, k_1 a positive constant and $\hat{\delta}_1$ the estimation of δ_1. Meanwhile, $\hat{\beta}_i$, $i=1$, 2 and $\hat{\delta}_1$ are learned in the following way.

$$\begin{aligned} \dot{\hat{\beta}}_1 &= \gamma_1 s_1 (c_1\dot{e}_z + \ddot{z}_d + g), \\ \dot{\hat{\beta}}_2 &= \gamma_2 s_1 \dot{z}, \\ \dot{\hat{\delta}}_1 &= \lambda_1 |s_1|, \end{aligned} \tag{19}$$

where γ_1, γ_2 and λ_1 are positive learning gains.

The first main result of the paper is summarized as follows:

Theorem 1: Consider the altitude dynamic model of the quadrotor in the form (9) and (15) with the controllers (18) and adaptive laws (19). Under Assumptions 1 and 2, the output tracking error of the altitude channel of the quadrotor system is guaranteed to converge to zero asymptotically, i.e., $e_z \to 0$ as $t \to \infty$.

Proof: Define the following Lyapunov function candidate:

$$V_z = \frac{1}{2}ms_1^2 + \frac{1}{2\gamma_1}\tilde{\beta}_1^2 + \frac{1}{2\gamma_2}\tilde{\beta}_2^2 + \frac{1}{2\lambda_1}\tilde{\delta}_1^2, \tag{20}$$

where the $\tilde{\delta}_1$ is the estimation error, defined as $\tilde{\delta}_1 = \delta - \hat{\delta}$. Then, the time derivative of V_z is

$$\dot{V}_z = ms_1\dot{s}_1 + \frac{1}{\gamma_1}\tilde{\beta}_1\dot{\tilde{\beta}}_1 + \frac{1}{\gamma_2}\tilde{\beta}_2\dot{\tilde{\beta}}_2 + \frac{1}{\lambda_1}\tilde{\delta}_1\dot{\tilde{\delta}}_1. \tag{21}$$

From (17), $\dot{s}_1$ in (21) can be calculated in the following way.

$$\begin{aligned} \dot{s}_1 &= c_1\dot{e}_z + \ddot{e}_z \\ &= c_1\dot{e}_z + \ddot{z}_d - \ddot{z}. \end{aligned} \tag{22}$$

Noticing the definition of $\tilde{d}_z$, (22) and the third equation in (9), we have

$$\begin{aligned} ms_1\dot{s}_1 =& ms_1(c_1\dot{e}_z + \ddot{z}_d - \ddot{z}) \\ =& s_1(m(c_1\dot{e}_z + \ddot{z}_d) - (U_1\cos\phi\cos\theta - k_z\dot{z} \\ &- mg + \tilde{d}_z)) \\ =& m(s_1(c_1\dot{e}_z + \ddot{z}_d + g)) + k_z s_1\dot{z} \\ &- s_1 U_1\cos\phi\cos\theta - s_1\tilde{d}_z. \end{aligned} \tag{23}$$

Considering the definitions of β_1 and β_2, substituting the altitude controller (18) into (23) renders to

$$\begin{aligned} ms_1\dot{s}_1 =& \beta_1 s_1(c_1\dot{e}_z + \ddot{z}_d + g) + \beta_2 s_1\dot{z} \\ &- \hat{\beta}_1(s_1(c_1\dot{e}_z + \ddot{z}_d + g) - \hat{\beta}_2 s_1\dot{z} \\ &- s_1\hat{\delta}_1 sgn(s_1) - k_1 s_1^2 - s_1\tilde{d}_z \\ =& \tilde{\beta}_1 s_1(c_1\dot{e}_z + \ddot{z}_d + g) + \tilde{\beta}_2 s_1\dot{z} \\ &- s_1\hat{\delta}_1 sgn(s_1) - k_1 s_1^2 - s_1\tilde{d}_z. \end{aligned} \tag{24}$$

Applying (24) into (21) yields

$$\begin{aligned} \dot{V}_z =& \tilde{\beta}_1 s_1(c_1\dot{e}_z + \ddot{z}_d + g) + \tilde{\beta}_2 s_1\dot{z} \\ &- s_1\hat{\delta}_1 sgn(s_1) - k_1 s_1^2 - s_1\tilde{d}_z \\ &+ \frac{1}{\gamma_1}\tilde{\beta}_1\dot{\tilde{\beta}}_1 + \frac{1}{\gamma_2}\tilde{\beta}_2\dot{\tilde{\beta}}_2 + \frac{1}{\lambda_1}\tilde{\delta}_1\dot{\tilde{\delta}}_1. \end{aligned} \tag{25}$$

Since $\dot{\tilde{\beta}}_1 = -\dot{\hat{\beta}}_1$, $\dot{\tilde{\beta}}_2 = -\dot{\hat{\beta}}_2$ and $\dot{\tilde{\delta}}_1 = -\dot{\hat{\delta}}_1$ by the definitions of $\tilde{\beta}_1$, $\tilde{\beta}_2$ and $\tilde{\delta}$, (25) can be rewritten as

$$\begin{aligned}\dot{V}_z =&\tilde{\beta}_1(s_1(c_1\dot{e}_z+\ddot{z}_d+g)-\frac{1}{\gamma_1}\dot{\hat{\beta}}_1)+\tilde{\beta}_2(s_1\dot{z}-\frac{1}{\gamma_2}\dot{\hat{\beta}}_2)\\ &-\frac{1}{\lambda_1}\tilde{\delta}_1\dot{\hat{\delta}}_1-s_1\hat{\delta}_1 sgn(s_1)-k_1s_1^2-s_1\tilde{d}_z. \end{aligned} \tag{26}$$

Invoking the adaptive laws of $\hat{\beta}_1$, $\hat{\beta}_2$ and $\hat{\delta}_1$ in (19) and adopting the relationship $|\tilde{d}_z| \le \delta_1$, (26) further gives

$$\begin{aligned}\dot{V}_z &= -\frac{1}{\lambda_1}\tilde{\delta}_1\dot{\hat{\delta}}_1-s_1\hat{\delta}_1 sgn(s_1)-s_1\tilde{d}_z-k_1s_1^2\\ &=-\frac{1}{\lambda_1}\tilde{\delta}_1\dot{\hat{\delta}}_1-\hat{\delta}_1|s_1|-s_1\tilde{d}_z-k_1s_1^2\\ &\le-\frac{1}{\lambda_1}\tilde{\delta}_1\dot{\hat{\delta}}_1-\hat{\delta}_1|s_1|+\delta_1|s_1|-k_1s_1^2\\ &\le-\frac{1}{\lambda_1}\tilde{\delta}_1\dot{\hat{\delta}}_1+\tilde{\delta}_1|s_1|-k_1s_1^2\\ &\le\tilde{\delta}_1(|s_1|-\frac{1}{\lambda_1}\dot{\hat{\delta}}_1)-k_1s_1^2\\ &\le -k_1s_1^2\\ &\le 0, \end{aligned} \tag{27}$$

implying that s_1 will converge to zero asymptotically. Observing the detailed expression of the sliding surface (17), the asymptotical convergence of s_1 directly gives that of e_z. □

3.2. Attitude controller design

Next, the design of roll, pitch and yaw controllers under the framework of ASMC will be presented in detail. First address the controller of roll channel.

Define sliding surface as

$$s_2 = c_2e_\phi+\dot{e}_\phi, \tag{28}$$

where c_2 is a controller parameter to be designed and $c_2 > 0$.

The control law U_2 of roll channel is designed by

$$U_2 = \hat{\delta}_2 sgn(s_2)+k_2s_2+\hat{\beta}_3(c_2\dot{e}_\phi+\ddot{\phi}_d)-\hat{\beta}_4\dot{\theta}\dot{\varphi}, \tag{29}$$

where k_2 is a positive constant and $\hat{\delta}_2$ is the estimation of δ_2. Then, the adaptive laws of $\hat{\beta}_i, i=3,4$ and $\hat{\delta}_2$ are designed as

$$\begin{aligned}\dot{\hat{\beta}}_3 &= \gamma_3 s_2(c_2\dot{e}_\phi+\ddot{\phi}_d),\\ \dot{\hat{\beta}}_4 &= -\gamma_4 s_2\dot{\theta}\dot{\varphi},\\ \dot{\hat{\delta}}_2 &= \lambda_2|s_2|, \end{aligned} \tag{30}$$

where γ_3, γ_4 and λ_2 are positive constants.

The second main result of the paper is summarized as follows.

Theorem 2: Consider the roll dynamic model of the quadrotor in the form (15) with the controllers (29) and adaptive laws (30). Under Assumption 1, the output tracking error of the roll channel of the quadrotor system is guaranteed to converge to zero asymptotically, i.e., $e_\phi \to 0$ as $t \to \infty$.

Proof: Considering the following candidate Lyapunov function:

$$V_\phi = \frac{1}{2}\frac{J_x}{L}s_2^2+\frac{1}{2\gamma_3}\tilde{\beta}_3^2+\frac{1}{2\gamma_4}\tilde{\beta}_4^2+\frac{1}{2\lambda_2}\tilde{\delta}_2^2, \tag{31}$$

where the $\tilde{\delta}_2$ is the estimation error, defined as $\tilde{\delta}_2 = \delta-\hat{\delta}$. Then, differentiating V_ϕ with respect to time yields:

$$\dot{V}_\phi = \frac{J_x}{L}s_2\dot{s}_2+\frac{1}{\gamma_3}\tilde{\beta}_3\dot{\tilde{\beta}}_3+\frac{1}{\gamma_4}\tilde{\beta}_4\dot{\tilde{\beta}}_4+\frac{1}{\lambda_2}\tilde{\delta}_2\dot{\tilde{\delta}}_2. \tag{32}$$

By (28), $\dot{s}_2$ in (32) satisfies

$$\begin{aligned}\dot{s}_2 &= c_2\dot{e}_\phi+\ddot{e}_\phi\\ &= c_2\dot{e}_\phi+\ddot{\phi}_d-\ddot{\phi}. \end{aligned} \tag{33}$$

Noticing the definition of $\tilde{d}_\phi$, using the first equation in (15) and (33), the first term on the right-hand side of (32) can be rewritten as

$$\begin{aligned}\frac{J_x}{L}s_2\dot{s}_2 =&\frac{J_x}{L}s_2(c_2\dot{e}_\phi+\ddot{\phi}_d-\ddot{\phi})\\ =&s_2(\frac{J_x}{L}(c_2\dot{e}_\phi+\ddot{\phi}_d)\\ &-(U_2+\frac{J_y-J_z}{L}\dot{\theta}\dot{\varphi}+\tilde{d}_\phi))\\ =&s_2\frac{J_x}{L}(c_2\dot{e}_\phi+\ddot{\phi}_d)-s_2\frac{J_y-J_z}{L}\dot{\theta}\dot{\varphi}\\ &-s_2U_2-s_2\tilde{d}_\phi. \end{aligned} \tag{34}$$

Considering the definitions of β_3 and β_4, and substituting the roll control input (29) into (34), we have

$$\begin{aligned}\frac{J_x}{L}s_2\dot{s}_2 =&\beta_3(s_2(c_2\dot{e}_\phi+\ddot{\phi}_d))-\beta_4s_2\dot{\theta}\dot{\varphi}\\ &-\hat{\beta}_3s_2(c_2\dot{e}_\phi+\ddot{\phi}_d)+\hat{\beta}_4s_2\dot{\theta}\dot{\varphi}\\ &-s_2\hat{\delta}_2 sgn(s_2)-k_2s_2^2-s_2\tilde{d}_\phi\\ =&\tilde{\beta}_3(s_2(c_2\dot{e}_\phi+\ddot{\phi}_d))-\tilde{\beta}_4s_2\dot{\theta}\dot{\varphi}\\ &-s_2\hat{\delta}_2 sgn(s_2)-k_2s_2^2-s_2\tilde{d}_\phi. \end{aligned} \tag{35}$$

Substituting (35) into (32) yields

$$\begin{aligned}\dot{V}_\phi =&\tilde{\beta}_3(s_2(c_2\dot{e}_\phi+\ddot{\phi}_d))-\tilde{\beta}_4s_2\dot{\theta}\dot{\varphi}\\ &+\frac{1}{\gamma_3}\tilde{\beta}_3\dot{\tilde{\beta}}_3+\frac{1}{\gamma_4}\tilde{\beta}_4\dot{\tilde{\beta}}_4+\frac{1}{\lambda_2}\tilde{\delta}_2\dot{\tilde{\delta}}_2\\ &-s_2\hat{\delta}_2 sgn(s_2)-s_2\tilde{d}_\phi-k_2s_2^2. \end{aligned} \tag{36}$$

Since $\dot{\tilde{\beta}}_3 = -\dot{\hat{\beta}}_3$, $\dot{\tilde{\beta}}_4 = -\dot{\hat{\beta}}_4$ and $\dot{\tilde{\delta}}_2 = -\dot{\hat{\delta}}_2$, it follows from (36) that

$$\begin{aligned}\dot{V}_\phi =&\tilde{\beta}_3(s_2(c_2\dot{e}_\phi + \ddot{\phi}_d) - \frac{1}{\gamma_3}\dot{\hat{\beta}}_3) - \tilde{\beta}_4(s_2\dot{\theta}\dot{\varphi} + \frac{1}{\gamma_4}\dot{\hat{\beta}}_4)\\ &- \frac{1}{\lambda_2}\tilde{\delta}_2\dot{\hat{\delta}}_2 - s_2\hat{\delta}_2 sgn(s_2) - s_2\tilde{d}_\phi - k_2 s_2^2. \end{aligned} \quad (37)$$

By substituting the adaptive laws (30) into (37) and employing the relationship $|\tilde{d}_\phi| \leq \delta_2$, we obtain

$$\begin{aligned}\dot{V}_\phi =&-\frac{1}{\lambda_2}\tilde{\delta}_2\dot{\hat{\delta}}_2 - s_2\hat{\delta}_2 sgn(s_2) - s_2\tilde{d}_\phi - k_2 s_2^2\\ =&-\frac{1}{\lambda_2}\tilde{\delta}_2\dot{\hat{\delta}}_2 - \hat{\delta}_2|s_2| - s_2\tilde{d}_\phi - k_2 s_2^2\\ \leq&-\frac{1}{\lambda_2}\tilde{\delta}_2\dot{\hat{\delta}}_2 - \hat{\delta}_2|s_2| + \delta_2|s_2| - k_2 s_2^2\\ \leq&-\frac{1}{\lambda_2}\tilde{\delta}_2\dot{\hat{\delta}}_2 + \tilde{\delta}_2|s_2| - k_2 s_2^2\\ \leq&\tilde{\delta}_2(|s_2| - \frac{1}{\lambda_2}\dot{\hat{\delta}}_2) - k_2 s_2^2\\ \leq&-k_2 s_2^2\\ \leq&0, \end{aligned} \quad (38)$$

indicating that s_2 will converge to zero asymptotically. Observing the detailed expression of the sliding surface (28), the asymptotical convergence of s_2 directly gives that of e_ϕ. □

Parallel to the way in designing the control and adaptive laws for the altitude and roll channels, the controller design for the pitch and yaw channels can be derived similarly and given directly in the following.

$$U_3 = \hat{\delta}_3 sgn(s_3) + k_3 s_3 + \hat{\beta}_5(c_3\dot{e}_\theta + \ddot{\theta}_d) - \hat{\beta}_6\dot{\phi}\dot{\varphi}, \quad (39)$$

$$\begin{aligned}&\dot{\hat{\beta}}_5 = \gamma_5 s_3(c_3\dot{e}_\theta + \ddot{\theta}_d),\\ &\dot{\hat{\beta}}_6 = -\gamma_6 s_3\dot{\phi}\dot{\varphi},\\ &\dot{\hat{\delta}}_3 = \lambda_3|s_3|, \end{aligned} \quad (40)$$

$$U_4 = \hat{\delta}_4 sgn(s_4) + k_4 s_4 + \hat{\beta}_7(c_4\dot{e}_\varphi + \ddot{\varphi}_d) - \hat{\beta}_8\dot{\phi}\dot{\theta}, \quad (41)$$

$$\begin{aligned}&\dot{\hat{\beta}}_7 = \gamma_7 s_4(c_4\dot{e}_\varphi + \ddot{\varphi}_d),\\ &\dot{\hat{\beta}}_8 = -\gamma_8 s_4\dot{\phi}\dot{\theta},\\ &\dot{\hat{\delta}}_4 = \lambda_4|s_4|, \end{aligned} \quad (42)$$

where c_i, k_i, λ_i, $i = 3,\ 4$, γ_j, $j = 5, \cdots, 8$ are positive constants and s_3, s_4 are the sliding surfaces, defined as $s_3 = c_3 e_\phi + \dot{e}_\phi$, $s_4 = c_4 e_\theta + \dot{e}_\theta$, respectively.

Remark 1: It is worth mentioning that, since the signum functions are involved in the controllers, chattering phenomenon could be serious when the proposed ASMC laws (18), (29), (39) and (41) are applied in the quadrotor UAV system. To resolve this, saturation functions are used to replace the signum functions in all four channels [42]. The resultant control performance has been verified via simulation and real experiment.

Remark 2: In experiments, measurement noise [9, 30] is inevitable in the feedback test of all state variables of quadrotors. The robustness of the proposed control algorithm to measurement noise will be illustrated in simulation experiments.

4. SIMULATION AND EXPERIMENTAL RESULTS

In this section, the simulation and experimental results of the three control algorithms including ASMC, LQR and ADRC are presented, respectively. Furthermore, some discussion and analysis of these results will be given.

4.1. Simulation

The numerical simulation results for ASMC, LQR and ADRC are first presented. The physical parameters of mathematical model of the quadrotor system and design parameters of ASMC are listed in Tables 1 and 2, respectively.

The initial altitude and attitude of the four-rotor system are assumed as 0 m and $[0,0,0]$ rad. The desired outputs of altitude and attitude channels are assumed to be $z_d =$

Table 1. Physical parameters of the quadrotor UAV [24].

Symbol	Value	Units
m	2.33	kg
g	9.8	m/s^2
l	0.4	m
I_x	0.16	kgm^2
I_y	0.16	kgm^2
I_z	0.32	kgm^2
k_x	0.008	N/m/s
k_y	0.008	N/m/s
k_z	0.012	N/m/s
f	0.05	m

Table 2. Controller parameters.

Variable	Value	Variable	Value
c_1	1	c_3	4
k_1	1000	k_3	20
γ_1	4	γ_5	3.2
γ_2	0.005	γ_6	15
λ_1	1.2	λ_3	1
c_2	4	c_4	4
k_2	20	k_4	1000
γ_3	3.2	γ_7	220
γ_4	10	γ_8	1
λ_2	1	λ_4	1.2

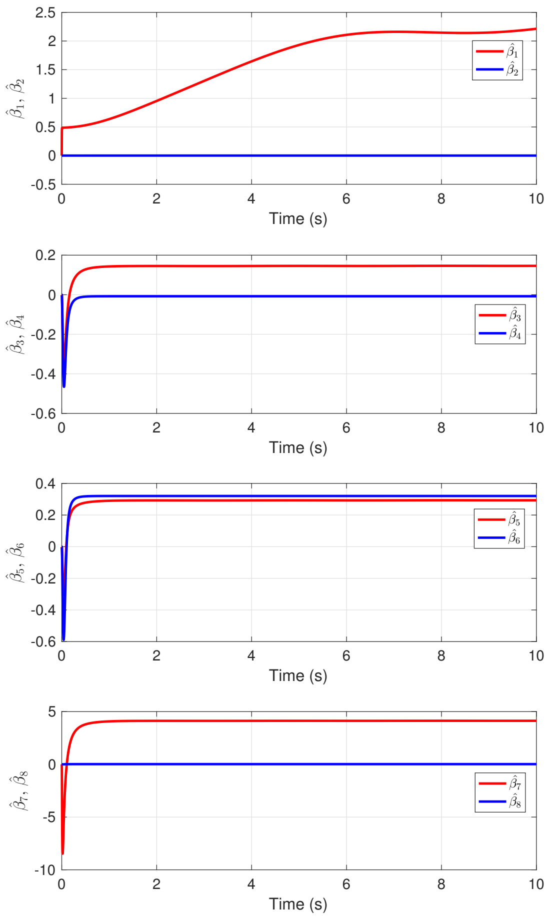

Fig. 3. The estimations of physical parameters.

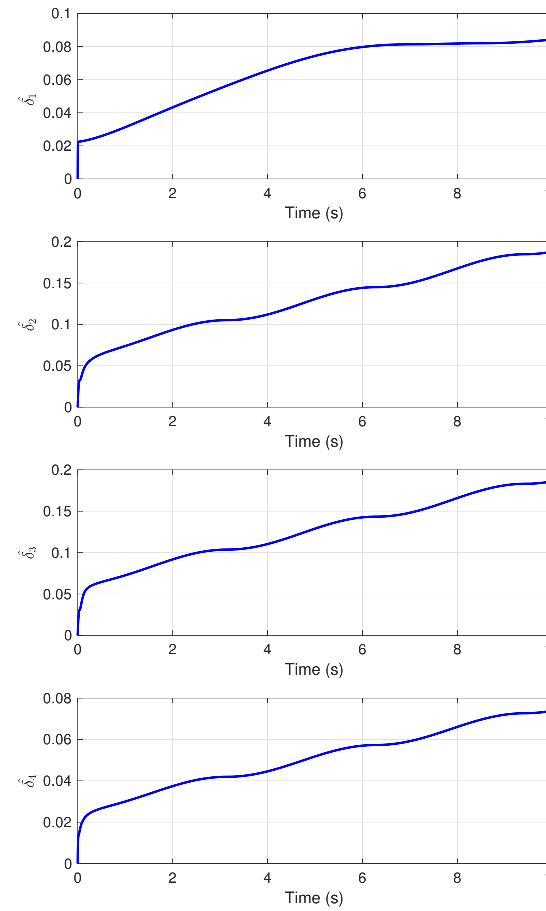

Fig. 4. The estimations of upper bounds of external disturbances.

8 m, $\phi_d = \theta_d = \varphi_d = 0.5$ rad, respectively. Besides, for the purpose of simulation, the external disturbances are chosen as $d_x = d_y = d_z = d_\phi = d_\theta = d_\varphi = \sin(t)$.

The physical parameters β_i, $i = 1, \cdots, 8$ and the upper bound of the external disturbance $\delta_i, i = 1, \cdots, 4$ are online estimated by (19), (30), (40) and (42), as shown in Figs. 3 and 4.

Fig. 5 depicts the time response of the outputs of ASMC, LQR and ADRC. It is obviously seen that the chattering phenomena is greatly suppressed when using the proposed control scheme, which means that the control signal can be easily applied in real system of quadrotor UAV.

To demonstrate the ability of the proposed control algorithm to track the reference signal, we now apply the control algorithms, i.e., ASMC, LQR and ADRC to complete the tracking of the given altitude and attitude. The simulation results are exhibited in Fig. 6, from which it can be observed that the altitude and attitude angles of the four-rotor UAV are stabilized close to the desired outputs by ASMC despite the external disturbance injecting along the z, ϕ, θ and φ directions. Although the tracking speed of LQR is faster, it produces a larger oscillation in altitude channel. Besides, it is clear that the tracking speed of ASMC is faster than that of ADRC. In attitude channel, the oscillation produced by LQR and ADRC is indeed larger than that produced by ASMC. Therefore, the tracking performance and the robustness of ASMC is better than that of LQR and ADRC.

Furthermore, to illustrate the robustness of the proposed control algorithm to measurement noise, as presented in Fig. 7, the simulations of the three control methods are conducted and the corresponding results are shown in Fig. 8. It can be seen that, compared with ASMC and ADRC, the measurement noise has a greater impact on control capability of LQR, and even the reference signal cannot be tracked in the roll and pitch channels. In addition, although there is a steady state error when ASMC is applied, the rise time of ASMC is shorter than that of ADRC in altitude channel. Meanwhile, as shown in Fig. 8, the control performance of ASMC is better than that of LQR and ADRC in terms of tracking accuracy in attitude channel when the measurement noise is involved.

Remark 3: In simulations, the controller parameters in Table 2 are debugged step by step based on the tracking

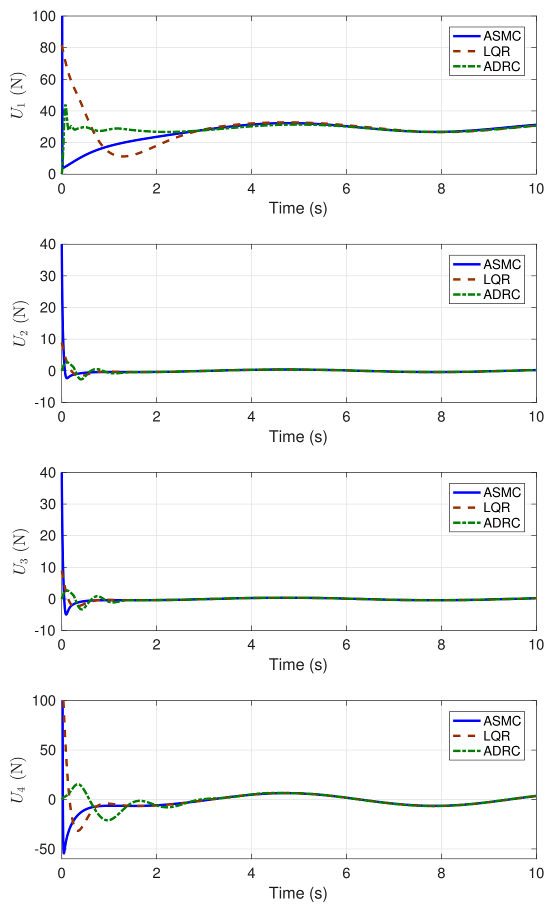

Fig. 5. The control input profiles for all the input channels.

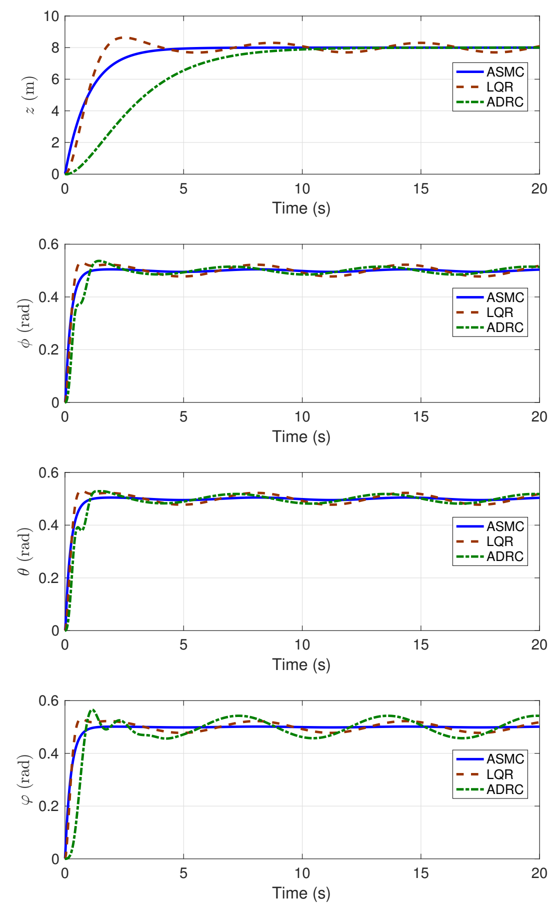

Fig. 6. The tracking performance of altitude and attitude.

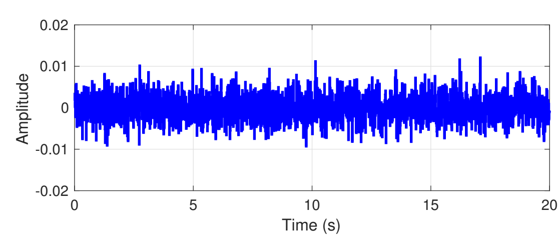

Fig. 7. The measurement noise.

results, and these parameters might not be the optimal parameters. It is found that c_i, $i = 1, \cdots, 4$ and k_i, $i = 1, \cdots, 4$ are the parameters that have a greater impact on the tracking results during debugging.

Remark 4: It is worth mentioning that the estimations of system physical parameters and the upper bound of external disturbances may not converge to their true values, since the estimation errors is not guaranteed to converge to zero when using the Lyapunov function to analyze the stability of the four-rotor system.

4.2. Experiment test

In experiment, the proposed control strategy is applied to a quadrotor UAV platform provided by Beijing Links Tech Co., Ltd., as shown in Fig. 9. This platform uses a personal computer (PC), a 51.5 cm $\times$ 51.5 cm test bench, an external DC power module, a power adapter, an USB to RS485 converter, a wind speed sensor and an AR Drone 2.0 quadrotor system with 1 GHz 32 bit ARM Cortex A8 processor, 3-axis gyroscope, 3-axis accelerometer, 3-axis magnetometer, barometer, ultrasonic sensor, 4 brushless motors, 4 motor controllers and a Wi-Fi wireless module. To ensure the test safety, the quadrotor is fixed on the test platform. Meanwhile, a strong electric fan is utilized to produce the sustained wind disturbance, whose speed can be measured by a wind speed sensor.

The power adapter and the external DC power module provide stable power supplies for the USB to RS485 converter and processor of the quadrotor, respectively. The controllers are first implemented in MATLAB/Simulink. Then the code generation technique provided by MATLAB is used to convert the Simulink model into C language code, which is downloaded to the processor via Wi-Fi. In addition, the tracking data collected by the sensors on the quadrotor system can also be transmitted back to MATLAB by Wi-Fi. The USB to RS485 converter is uti-

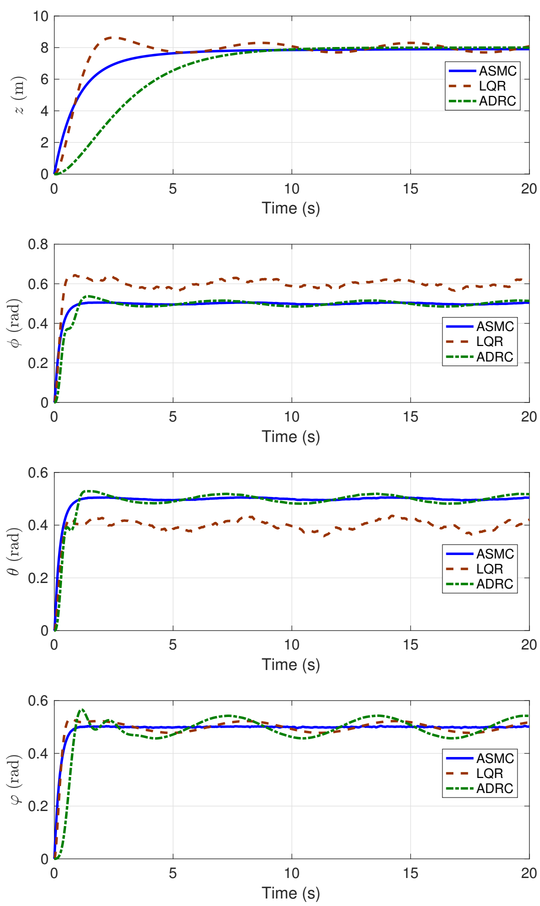

Fig. 8. The tracking performance of altitude and attitude under measurement noise.

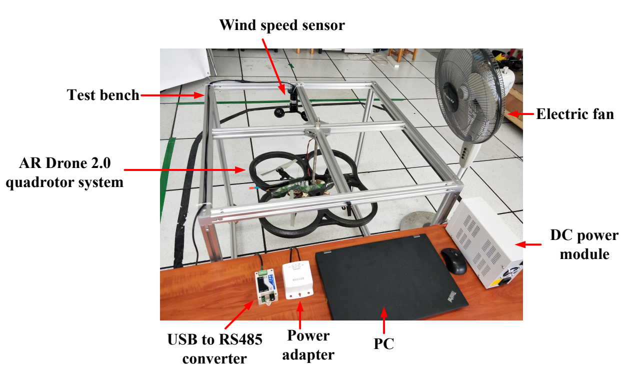

Fig. 9. Quadrotor UAV platform.

lized to transmit the wind speed to the monitoring software of the PC. Therefore, we can observe the tracking results for the reference signal and the speed of external wind disturbance in real time on the PC. It is worth noting that the altitude controller is not verified in the experiment, since the altitude of the quadrotor is fixed.

Two experiments with different wind speeds have been performed on the quadrotor platform. Notice that the initial attitudes of the quadrotor could be different in the actual tests, since the attitude of the quadrotor cannot be measured when the quadrotor is in the stationary state.

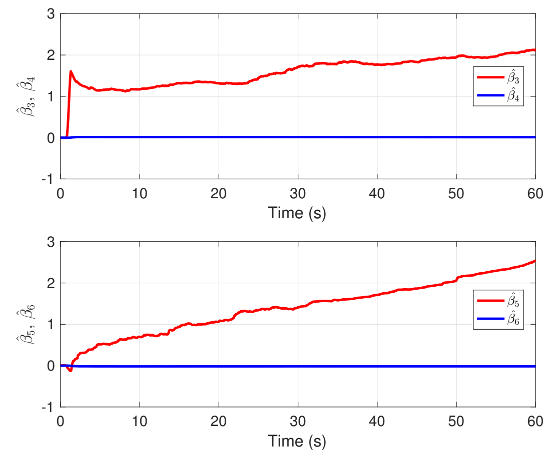

Fig. 10. The estimations of physical parameters under the wind speed of 2.7 m/s.

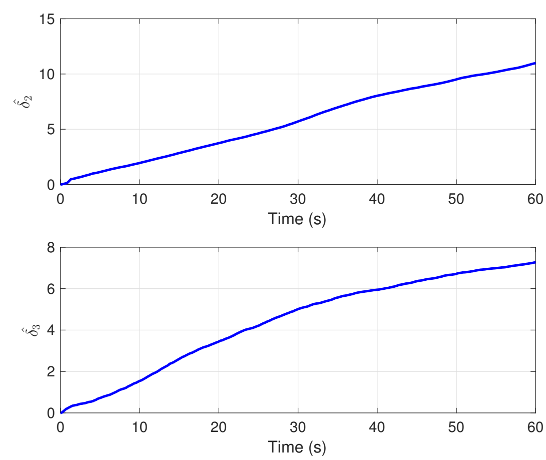

Fig. 11. The estimations of upper bounds of external disturbances under the wind speed of 2.7 m/s.

Case 1: The control objective is to stabilize the attitude of the quadrotor at 0 rad under the wind speed of 2.7 m/s.

The estimation of physical parameters β_i, $i = 3, \cdots, 6$ and upper bounds of external disturbance δ_i, $i = 2, \cdots, 3$ are plotted in Figs. 10-11.

The controller outputs of roll and pitch dynamics systems are presented in Fig. 12. The experiment results of roll and pitch channels are provided in Fig. 13. In view of these results, notice that ADRC produces a larger oscillation at the beginning of the flight test, and then achieves a stable tracking for the reference signal. Meanwhile, ASMC and LQR give an almost equal control effect for the tracking of roll and pitch angles. The tracking errors of the three control algorithms remain in a small neighborhood of zero when the flight time of the quadrotor exceeds 15 seconds.

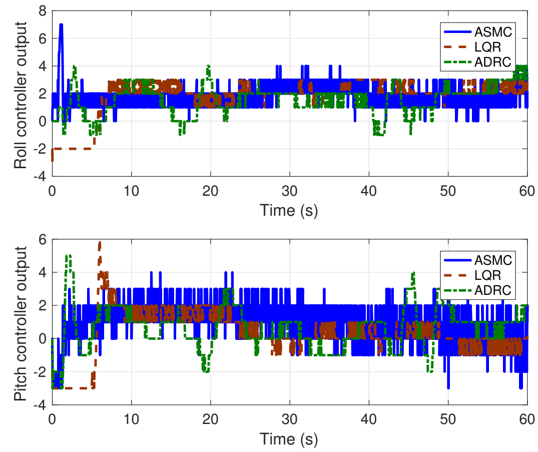

Fig. 12. The outputs of the roll and pitch controllers under the wind speed of 2.7 m/s.

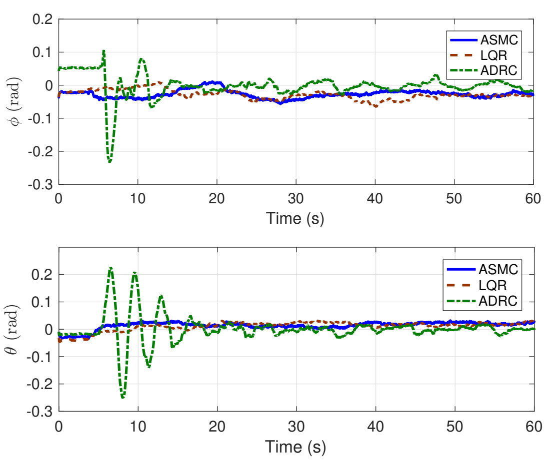

Fig. 13. Tracking results of roll and pitch angles under the wind speed of 2.7 m/s.

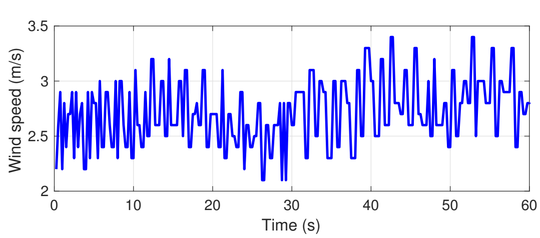

Fig. 14. Time-varying wind speed.

Case 2: The task of the reference tracking of the attitude angle of 0 rad is assigned for the quadrotor under the time-varying wind speed, as shown in Fig. 14.

The Figs. 15-16 show the online estimation for the controller parameters β_i, $i = 3, \cdots, 6$ and upper bounds of external disturbance δ_i, $i = 2, \cdots, 3$.

Fig. 17 depicts the controller outputs of the three algorithms in the movements of roll and pitch. Fig. 18 presents

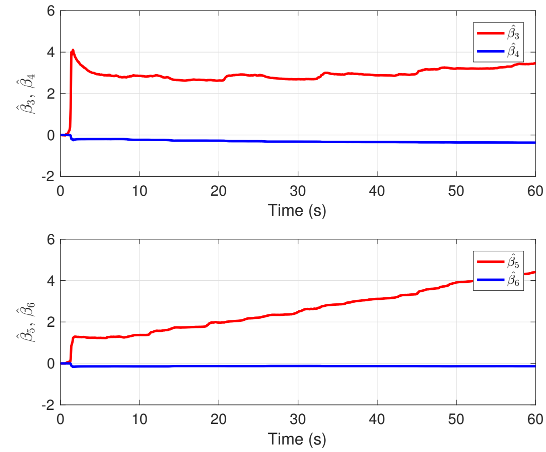

Fig. 15. The estimations of physical parameters under the time-varying wind speed.

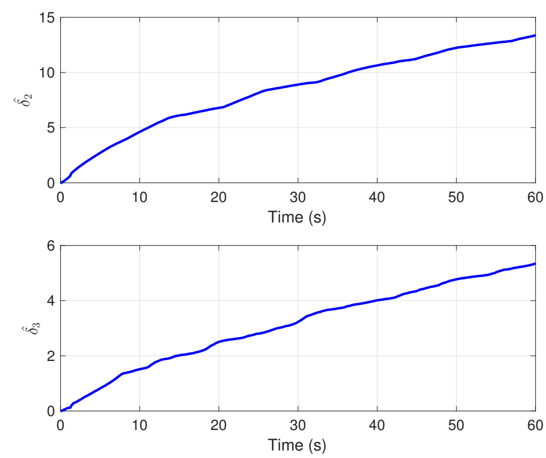

Fig. 16. The estimations of upper bounds of external disturbances under the time-varying wind speed.

the time history of the tracking for the desired roll and pitch angles of the quadrotor. It is clear that there is a larger oscillation in the roll and pitch channels throughout the flight test when applying ADRC to the quadrotor platform, which could be reduced by adjusting the parameters of the ADRC. Besides, the tracking error of LQR is larger than that of ASMC in roll channel, while the tracking performance of ASMC and LQR for the reference signal is almost same, as shown in pitch channel in Fig. 18.

From the experimental results of Figs. 13 and 18, we can conclude that the control performance of ASMC is indeed better than that of LQR and ADRC under the effect of constant or time-varying wind speed.

Remark 5: It is worth noting that the outputs of the controllers are U_i, $i = 1, \cdots, 4$ of (9) and (15) in simulation. However, the outputs of the controllers are constant scalars to be used for calculating the duty cycle of voltage in the processor of the actual experiment.

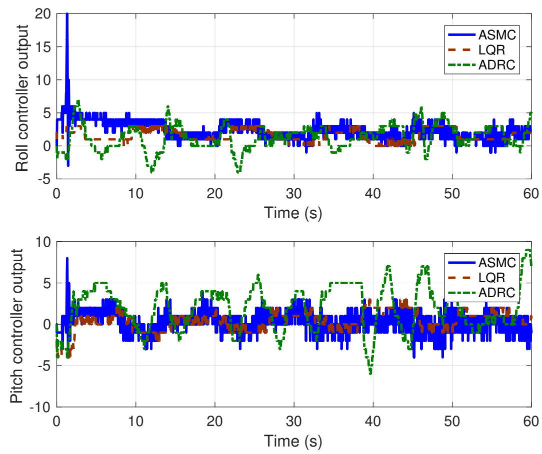

Fig. 17. The outputs of the roll and pitch controllers under the time-varying wind speed.

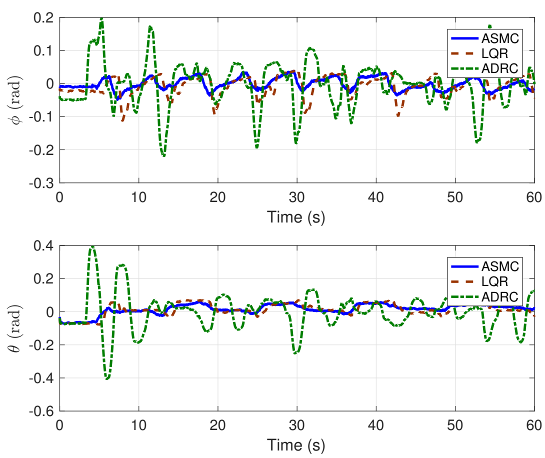

Fig. 18. Tracking results of roll and pitch angles under the time-varying wind speed.

Remark 6: Indeed, the proposed control method is more complex than LQR and ADRC algorithms in terms of controller structure and the number of parameter. However, the proposed controller has better robustness against external disturbances, which has been proven by simulation and experiment. In addition, parameter tuning of the proposed method is easier and more regular than that of LQR and ADRC. As a result, the proposed algorithm can be easily applied to the actual UAV system and the effectiveness of the proposed algorithm would be verified accordingly.

5. CONCLUSION

This paper studies the altitude and attitude tracking control problems for a quadrotor UAV system subject to parametric uncertainties and external disturbances. To enable the designed controller to be applied to any quadrotor, all parameters of the quadrotor dynamics are estimated by the designed adaptive laws. The stability of the closed-loop system has been proven by Lyapunov theory. Furthermore, the tracking errors of altitude and attitude of the quadrotor system are guaranteed to converge to zero asymptotically. Moreover, simulations and real experiments of ASMC, LQR and ADRC are conducted respectively to illustrate the superiority of the proposed control scheme in effectiveness and robustness. We will focus on finite-time stability of a quadrotor UAV subject to input saturation and develop a nonlinear disturbance observer to compensate for external disturbance in future research.

REFERENCES

[1] D. Cabecinhas, R. Naldi, L. Marconi, C. Silvestre, and R. Cunha, "Robust take-off for a quadrotor vehicle," *IEEE Transactions on Robotics*, vol. 28, no. 3, pp. 734-742, June 2012.

[2] Y. C. Choi and H. S. Ahn, "Nonlinear control of quadrotor for point tracking: actual implementation and experimental tests," *IEEE/ASME Transactions on Mechatronics*, vol. 20, no. 3, pp. 1179-1192, June 2015.

[3] H. Wei and B. Xian, "Nonlinear adaptive fault-tolerant control for a quadrotor UAV based on immersion and invariance methodology," *Nonlinear Dynamics*, vol. 90, no. 10, pp. 1-14, December 2017.

[4] A. Ailon and S. Arogeti, "Closed-form nonlinear tracking controllers for quadrotors with model and input generator uncertainties," *Automatica*, vol. 54, no. C, pp. 317-324, April 2015.

[5] M. E. Guerrero-Sánchez, D. A. Mercado-Ravell, L. Rogelio, and C. D. García-Beltrán, "Swing-attenuation for a quadrotor transporting a cable-suspended payload," *ISA Transactions*, vol. 68, pp. 433-449, May 2017.

[6] T. Lee, "Robust adaptive attitude tracking on SO(3) with an application to a quadrotor UAV," *IEEE Transactions on Control Systems Technology*, vol. 21, no. 5, pp. 1924-1930, September 2013.

[7] C. Ha, Z. Zuo, F. B. Choi, and D. Lee, "Passivity-based adaptive backstepping control of quadrotor-type UAVs," *Robotics and Autonomous Systems*, vol. 62, no. 9, pp. 1305-1315, September 2014.

[8] Y. Zou and B. Zhu, "Adaptive trajectory tracking controller for quadrotor systems subject to parametric uncertainties," *Journal of the Franklin Institute*, vol. 354, no. 15, pp. 6724-6746, October 2017.

[9] O. Mofid and S. Mobayen, "Adaptive sliding mode control for finite-time stability of quad-rotor UAVs with parametric uncertainties," *ISA Transactions*, vol. 72, pp. 1-14, January 2018.

[10] F. Chen, W. Lei, K. Zhang, G. Tao, and B. Jiang, "A novel nonlinear resilient control for a quadrotor UAV via backstepping control and nonlinear disturbance observer," *Nonlinear Dynamics*, vol. 85, no. 2, pp. 1281-1295, April 2016.

[11] M. A. M. Basri, "Trajectory tracking control of autonomous quadrotor helicopter using robust neural adaptive backstepping approach," *Journal of Aerospace Engineering*, vol. 31, no. 2, pp. 04017091-1-04017091-15, March 2018.

[12] Z. Jia, J. Yu, and Y. Mei, "Integral backstepping sliding mode control for quadrotor helicopter under external uncertain disturbances," *Aerospace Science and Technology*, vol. 68, pp. 299-307, September 2017.

[13] F. Muñoz, I. González-Hernández, S. Salazar, E. S. Espinoza, and R. Lozano, "Second order sliding mode controllers for altitude control of a quadrotor UAS: Real-time implementation in outdoor environments," *Neurocomputing*, vol. 233, pp. 61-71, April 2017.

[14] Y. R. Tang, X. Xiao, and Y. Li, "Nonlinear dynamic modeling and hybrid control design with dynamic compensator for a small-scale UAV quadrotor," *Measurement*, vol. 109, pp. 51-64, October 2017.

[15] H. Ríos, J. González-Sierra, and A. Dzul, "Robust tracking output-control for a quad-rotor: A continuous sliding-mode approach," *Journal of the Franklin Institute*, vol. 354, no. 15, pp. 6672-6691, October 2017.

[16] H. Ríos, R. Falcón, O. A. González, and A. Dzul, "Continuous sliding-mode control strategies for quadrotor robust tracking: Real-time application," *IEEE Transactions on Industrial Electronics*, vol. 66, no. 2, pp. 1264-1272, February 2019.

[17] Y. Liu, S. Rajappa, J. M. Montenbruck, P. Stegagno, H. Bülthoff, F. Allgöwer, and A. Zell, "Robust nonlinear control approach to nontrivial maneuvers and obstacle avoidance for quadrotor UAV under disturbances," *Robotics and Autonomous Systems*, vol. 98, pp. 317-332, December 2017.

[18] B. Xiao and S. Yin, "A new disturbance attenuation control scheme for quadrotor unmanned aerial vehicles," *IEEE Transactions on Industrial Informatics*, vol. 13, no. 6, pp. 2922-2932, December 2017.

[19] H. S. Kim, J. B. Park, and Y. H. Joo, "A systematic approach to fuzzy-model-based robust H_∞ control design for a quadrotor UAV under imperfect premise matching," *International Journal of Fuzzy Systems*, vol. 19, no. 4, pp. 1227-1237, August 2017.

[20] A. Poutney, C. Kennedy, G. Clayton, and H. Ashrafiuon, "Robust tracking control of quadrotors based on differential flatness: Simulations and experiments," *IEEE/ASME Transactions on Mechatronics*, vol. 23, no. 3, pp. 1126-1137, June 2018.

[21] K. Alexis, G. Nikolakopoulos, and A. Tzes, "Switching model predictive attitude control for a quadrotor helicopter subject to atmospheric disturbances," *Control Engineering Practice*, vol. 19, no. 10, pp. 1195-1207, October 2011.

[22] Q. Xu, Z. Wang, and Z. Zhen, "Information fusion estimation-based path following control of quadrotor UAVs subjected to Gaussian random disturbance," *ISA Transactions*, vol. 99, pp. 84-94, April 2019.

[23] G. V. Raffo, M. G. Ortega, and F. R. Rubio, "An integral predictive/nonlinear H_∞ control structure for a quadrotor helicopter," *Automatica*, vol. 46, no. 1, pp. 29-39, January 2010.

[24] Z. Xu, X. Nian, H. Wang, and Y. Chen, "Robust guaranteed cost tracking control of quadrotor UAV with uncertainties," *ISA Transactions*, vol. 69, pp. 157-165, July 2017.

[25] H. Liu, J. Xi, and Y. Zhong, "Robust attitude stabilization for nonlinear quadrotor systems with uncertainties and delays," *IEEE Transactions on Industrial Electronics*, vol. 64, no. 7, pp. 5585-5594, July 2017.

[26] S. Li, Y. Wang, and J. Tan, "Adaptive and robust control of quadrotor aircrafts with input saturation," *Nonlinear Dynamics*, vol. 89, no. 1, pp. 255-265, July 2017.

[27] X. Shao, J. Liu, H. Cao, C. Shen, and H. Wang, "Robust dynamic surface trajectory tracking control for a quadrotor UAV via extended state observer," *International Journal of Robust and Nonlinear Control*, vol. 28, no. 7, pp. 2700-2719, May 2018.

[28] Y. Bouzid, H. Siguerdidjane, and Y. Bestaoui,, "Nonlinear internal model control applied to VTOL multi-rotors UAV," *Mechatronics*, vol. 47, pp. 49-66, November 2017.

[29] B. Tian, L. Liu, H. Lu, Z. Zuo, Q. Zong, and Y. Zhang, "Multivariable finite time attitude control for quadrotor UAV: Theory and experimentation," *IEEE Transactions on Industrial Electronics*, vol. 65, no. 3, pp. 2567-2577, March 2018.

[30] M. Labbadi and M. Cherkaoui, "Robust adaptive nonsingular fast terminal sliding-mode tracking control for an uncertain quadrotor UAV subjected to disturbances," *ISA Transactions*, vol. 99, pp. 290-304, April 2019.

[31] M. Labbadi and M. Cherkaoui, "Robust adaptive backstepping fast terminal sliding mode controller for uncertain quadrotor UAV," *Aerospace Science and Technology*, vol. 93, pp. 1-14, October 2019.

[32] T. Huang, D. Huang, Z. Wang, and A. Shah, "Robust tracking control of a quadrotor UAV based on adaptive sliding mode controller," *Complexity*, vol. 2019, pp. 1-15, December 2019.

[33] Y. Huang, Z. Zheng, and L. Sun, "Saturated adaptive sliding mode control for autonomous vessel landing of a quadrotor," *IET Control Theory and Applications*, vol. 12, no. 13, pp. 1830-1842, September 2018.

[34] H. Razmi and S. Afshinfar, "Neural network-based adaptive sliding mode control design for position and attitude control of a quadrotor UAV," *Aerospace Science and Technology*, vol. 9, pp. 12-27, August 2019.

[35] L. Martins, C. Cardeira, and P. Oliveira, "Linear quadratic regulator for trajectory tracking of a quadrotor," *Proc. of the 21st International Federation of Automatic Control Symposium on Automatic Control in Aerospace*, pp. 176-181, August 2019.

[36] Y. Zhang, Z. Chen, X. Zhang, Q. Sun, and M. Sun, "A novel control scheme for quadrotor UAV based upon active disturbance rejection control," *Aerospace Science and Technology*, vol. 79, pp. 601-609, August 2018.

[37] M. Walid, N. Slaheddine, A. Mohamed, and B. Lamjed, "Modeling and control of a quadrotor UAV," *Proc. of the 15th International Conference on Sciences and Techniques of Automatic Control and Computer Engineering*, pp. 343-348, December 2014.

[38] K. Chang, Y. Xia, K. Huang, and D. Ma, "Obstacle avoidance and active disturbance rejection control for a quadrotor," *Neurocomputing*, vol. 190, no. 19, pp. 60-69, May 2016.

[39] F. Chen, R. Jiang, K. Zhang, B. Jiang, and G. Tao, "Robust backstepping sliding mode control and observer-based fault estimation for a quadrotor UAV," *IEEE Transactions on Industrial Electronics*, vol. 63, no. 8, pp. 5044-5056, August 2016.

[40] J. J. Xiong and G. B. Zhang, "Global fast dynamic terminal sliding mode control for a quadrotor UAV," *ISA Transactions*, vol. 66, pp. 233-240, January 2017.

[41] G. Perozzi, D. Efimov, J. M. Biannic, and L. Planckaert, "Trajectory tracking for a quadrotor under wind perturbations: Sliding mode control with state-dependent gains," *Journal of the Franklin Institute*, vol. 355, no. 12, pp. 4809-4838, August 2018.

[42] B. Abci, G. Zheng, D. Efimov, and M. E. B. El Najjar, "Robust altitude and attitude sliding mode controllers for quadrotors," *Proc. of the 20th International Federation of Automatic Control World Congress*, pp. 2720-2725, July 2017.

Tianpeng Huang received his B.S. degree in automation from Chongqing University of Science and Technology, Chongqing, China, in 2014, an M.S. degree in control science and engineering from Chongqing University of Posts and Telecommunications, Chongqing, China, in 2017. He is currently working toward a Ph.D. degree in control science and engineering at Southwest Jiaotong University, Chengdu, China. His research interests include quadrotor UAV, adaptive control, sliding mode control, nonlinear control and deep learning.

Deqing Huang received his B.S. and Ph.D. degrees in applied mathematics from the Mathematical College, Sichuan University, Chengdu, China, in 2002 and 2007, respectively, and the second Ph.D. degree in control engineering from National University of Singapore (NUS), Singapore in 2011. From 2010 to 2013, he was a Research Fellow in the Department of Electrical and Computer Engineering, NUS. From 2013 to 2016, he was a Research Associate in the Department of Aeronautics, Imperial College London, London, U.K. In January 2016, he joined the Department of Electronic and Information Engineering, Southwest Jiaotong University, Chengdu, as a Professor and the Department Head. His research interests include the areas of modern control theory, fluid system analysis and control, convex optimization, and robotics.

Zhikai Wang received his B.S. degree in electronic and information engineering from Southwest Jiaotong University, Chengdu, China, in 2020. He is currently working toward an M.S. degree in control science and engineering at Harbin Institute of Technology, Harbin, China. His research interests include quadrotor UAV, robotics, control and motion planning

Xi Dai received her B.S. degree in electrical engineering and automation from Shangqiu Normal University, Shangqiu, China, in 2017. She is currently working toward an M.S. degree in control theory and application at the School of Electrical Engineering, Southwest Jiaotong University, Chengdu, China. Her research interests include quadrotor UAV, image processing and machine learning.

Awais Shah received his B.S. degree in electrical engineering from Comsats University, Abbottabd, Pakistan in 2010, and an M.S. degree in electrical engineering from the School of Electrical Engineering, University of Bradford, England in 2012. He is currently a Ph.D. candidate in the School of Electrical Engineering, Southwest Jiaotong University, Chengdu, China. His research interests include intelligent control theory, sliding mode control, HVAC system.

Publisher's Note Springer Nature remains neutral with regard to jurisdictional claims in published maps and institutional affiliations.